Refereed Proceedings

The 13th International Conference on Fluidization - New Paradigm in Fluidization Engineering

Engineering Conferences International *Year* 2010

DECAY FACTOR WITH EXPERIMENTAL VARIABLES IN TWO CIRCULATING FLUIDIZED BED (CFB) RISERS

DongHyun Lee* Hyun Suk Lee† Jong Hun Lim‡
Sang Soon Park** Ho Jeong Chae†† Soon Yong Jeong‡‡

*Sungkyunkwan University, dhlee@skku.edu
†Korea Research Institute of Chemical Technology
‡Korea Research Institute of Chemical Technology
**Korea Research Institute of Chemical Technology
††SungKyunKwan University
‡‡SungKyunKwan University

DECAY FACTOR WITH EXPERIMENTAL VARIABLES IN TWO CIRCULTATING FLUIDIZED BED (CFB) RISERS

Hyun Suk Lee[1], Jong Hun Lim[1], Sang Soon Park[1,2], Ho Jeong Chae[2], Soon Yong Jeong[2], Dong Hyun Lee[1,*]
Department of Chemical Engineering, SungKyunKwan University,
300 Chunchun, Jangan, Suwon 440-746, Republic of Korea
[1] Alternative Chemicals/Fuel Research Centre, Korea Research Institute of Chemical Technology, P.O. Box 107, Yuseong-gu, Daejeon 305-600, Republic of Korea
T: +82-31-290-7340, Fax. +82-31-290-4709, E-mail. dhlee@skku.edu

ABSTRACT
The effects of the riser inlet velocity, solid mass flux and particle size on the axial solid holdup profile and decay factor were investigated using two circulating fluidized beds (CFBs) with FCC (Geldart A) particles as the bed materials. Based on the experimental results from the two-CFBs, the axial solid holdup in the two CFBs were compared with the correlations of previous studies. Also, an empirical correlation was proposed for decay factor that exhibited a good agreement with experimental data.

INTRODUCTION
Circulating fluidized beds (CFBs) operating in the fast fluidization regime with high gas-solid mass transfers and low-pressure drops have been utilized in numerous petrochemical industries for FCC (fluid catalytic cracking), coal combustion, and various catalytic reactions, including the methanol to olefins (MTO) process (1). CFB catalytic reactors utilize Geldart A group particles and operate at a high gas velocity and high solid circulation rate. On the other hand, CFB combustors, using Geldart B group particles, operate at lower gas velocities and solid circulation rates (2). Understanding the solid distribution and flow pattern in CFB risers is the key to the successful design and scale-up of a CFB system (3). Matsen (4) reported that "scale-up is still not an exact science, but is rather a mix of physics, mathematics, witchcraft, history and common sense that we call engineering". The axial solid holdup distribution in a riser was found to be dependent on the gas flow rate and solid mass flux as well as the inert particle properties, riser inlet diameter and height of the apparatus (5). Many studies on various aspects of CFB hydrodynamics have been reported (6, 7, 8). Many believe that the axial solid holdup profile in a riser typically represents an S-shape profile combining the dense phase at the bottom of the riser and a dilute phase at the top. However, other experiments did not show a S-shape profile. Therefore, the design and scale-up of CFB reactors are by no means easy tasks, particularly when the circulation of solids is involved. Li and Kwauk (9) first demonstrated the S-shape solid holdup profile with an inflection point in a fast fluidized bed. Hartge et al. (10) measured the axial solid holdup profile using a γ-ray absorption method to confirm the axial solid holdup profile that was well described by Li and Kwauk (9). Kato et al.(11) determined the height of the inflection point from the height where the 2nd differential coefficient of the axial pressure profile curve equals zero, and equation for the empirical correlation for the inflection point. There are several experimental results and empirical correlations for understanding the axial solid holdup profile of cold-mode CFB with many variables. Despite the necessity of being able to design lab-scale CFB reactors to work in CFB applications, there are insufficient experimental data for a small scale CFB design in the literature. Therefore, this study examined hydrodynamic scale-up factors for MTO process, such as the solid residence time and decay factor, in two-

Published by ECI Digital Archives, 2010

small scale (0.009 m-ID x 1.9 m-high and 0.0254 m-ID x 4 m-high) cold-bed CFBs and compared the experimental value with the existing correlations to confirm the validity on the conditions in two small scale CFBs.

EXPERIMENTAL

The experiments were carried out in two (0.009m-ID x 1.9 m-high and 0.0254m-ID x 4m-high) cold-type CFBs. The CFBs consisted of a riser, a bubbling bed, a cyclone and bag filter to separate the fine particles and a non-mechanical valve. The components were made from a transparent acrylic column equipped with a seal-pot, as a non-mechanical valve for the return of entrained particles. Fig. 1 shows the schematic diagram of the experimental apparatus in two (0.009m-ID x 1.9 m-high and 0.0254m-ID x 4m-high) cold-type CFBs. For smooth solid circulation, air was injected individually into four parts (riser, seal-pot, bubbling bed and seal-pot dipleg). All parts of the equipment were connected to copper lines and grounded. The pressure taps were mounted flush on the column and covered with a 250-mesh screen to prevent the particles from entering. The pressure transducer (Cole-Parmer Co., C-68071-12) was calibrated using a U-tube manometer and the pressure drops were converted to a current signal. A/D converter (COMI-ZOA, SD202) was connected to a PC to read the continuous pressure drop in the riser and convert the current to a voltage at 1 Hz for 200 s. The bubbling bed was filled with FCC particles and used as inert particles. Table 1 lists the physical properties of the solid particles. The ball valve was installed between the bottom of the cyclone and bubbling bed to measure the solid mass flux of the solids circulated based on a height of accumulated particles, time period and bulk density. To evaluate the hydrodynamics, including the axial solid holdup in a riser and solid mass flux, a steady-state was maintained in all experiments and carried out according to Table 2.

THEORY

Axial solid hold-up in a riser.

The axial solid holdup in the riser was determined by measuring the pressure differences on the riser height. The solid holdup can be expressed as follows:

$$\frac{\Delta P_r}{\Delta Z} = \rho_S \varepsilon_S g \tag{1}$$

Average solid residence time in a riser.

The average solid residence time in a riser was calculated by ΔP_r and the solid mass flux on the experimental variables. Assuming that the riser has no dead or bypass zones, the mean solid residence time in a riser can be calculated as follows (12):

$$\bar{t}_{res} = \frac{A \times Z}{A \times G_s / [\rho_s (1 - \bar{\varepsilon})]} \tag{2}$$

Decay factor in a riser.

In Fig. 2, Kunii and Levenspiel (14) proposed a free-entrainment model to estimate the decay factor in a riser, and used it to represent the axial solid holdup profile in the fast fluidized bed as follows:

$$\frac{\varepsilon_s - \overline{\varepsilon_s}^{*}}{\varepsilon_{sd} - \varepsilon_s^{*}} = \exp(-aZ_f) \tag{3}$$

The axial solid hold-up with the axial riser height can be expressed as follows:

$$\varepsilon_s = \varepsilon_s^* + (\varepsilon_{sd} - \varepsilon_s^*)\exp(-aZ_f) \quad (4)$$

The axial solid hold-up at the exit of riser can be expressed as

$$\varepsilon_{se} = \varepsilon_s^* + (\varepsilon_{sd} - \varepsilon_s^*)\exp(-aZ_e) \quad (5)$$

$$\varepsilon_{se} = G_s / [\rho_s \times (U_r - U_t)] \quad (6)$$

The mean axial solid hold-up at the entrainment region of Z_f is

$$\overline{\varepsilon_s} = \frac{1}{z_e}\int_0^{z_e} \varepsilon_s dZ_f \quad (7)$$

Inserting Eq. (4) into (7) and integrating gives

$$\overline{\varepsilon_s} = \varepsilon_s^* + \frac{\varepsilon_{sd} - \varepsilon_s^*}{aZ_e}[1 - \exp(-aZ_1)] = \varepsilon_s^* + \frac{\varepsilon_{sd} - \varepsilon_{se}}{aZ_e} \quad (8)$$

The decay factor is dependent on the operating conditions and physical properties of the bed materials. Adánez et al. (19) and Lei and Horio (20) proposed the following correlations of [Eq. (9) and Eq.(10)], respectively.

$$a(U_r - U_t)^2 D_r^{0.6} = 0.88 - 420 d_p \quad (9)$$

$$aD_r = 0.019\left(\frac{G_s}{U_r \rho_g}\right)^{-0.22}\left(\frac{U_r}{\sqrt{gD_r}}\right)^{-0.32}\left(\frac{\rho_p - \rho_g}{\rho_g}\right)^{0.41} \quad (10)$$

Bai and Kato (21) proposed the following correlations [Eqs. (11) and (12)] for ε_{sd} and ε_s^* in case of $G_s < G_s^*$

$$\frac{\varepsilon_{sd}}{\varepsilon_{se}} = 1 + 6.14\times10^{-3}\left(\frac{U_r}{G_s/\rho_s}\right)^{-0.23}\left(\frac{\rho_p - \rho_g}{\rho_g}\right)^{1.21}\left(\frac{U_r}{\sqrt{gD_r}}\right)^{-0.383} \quad (11)$$

$$\varepsilon_s^* = 4.04\varepsilon_{se}^{1.214} \quad (12)$$

Kunii and Levenspiel (26) proposed the equation to describe the deviation affected by riser exit.

$$\Delta\varepsilon_{sr} = C_e \varepsilon_{se} \exp[-a_e(H_f - z_f)) \quad (13)$$

Kim et al. (27) proposed for decay factor and reflux constant in Eqs (14~15) based on Eq(10).

$$a_e D_r = 1.27\left[\frac{(U_g - U_t)^2}{gD_r}\right]^{1/2}\left[\frac{G_s}{\rho_p(U_g - U_t)}\right]^{-1/2}\left[\frac{D_e}{D_r}\right]^{-1/2}\left[\frac{\rho_p - \rho_g}{\rho_g}\right]^{-1} \quad (14)$$

with a correlation coefficient of 0.90 and a standard error of estimate of 1.73.

$$C_e = 0.046\left[\frac{(U_g - U_t)^2}{gD_r}\right]^{1/2}\left[\frac{G_s}{\rho_p(U_g - U_t)}\right]^{-1/3}\left[\frac{H_e}{d_p}\right]^{1/3}\left[\frac{D_e}{D_r}\right]^{-3/4} \quad (15)$$

With a correlation coefficient of 0.92 and a standard error of estimate of 0.012.

RESULTS AND DISCUSSION

Fig. 3 shows the change in the axial solid hold-up profile with the dimensionless height including the data from previous studies. The axial solid holdup in the riser was determined by measuring pressure differences according to the riser height. The axial solid holdup can be calculated using Eq. (1) with the measured pressure drop along the axial riser height. The axial solid holdup in a riser is affected by the operating conditions, such as gas velocity, solid mass flux, particle properties, bed geometry, diameter of riser and exit geometry in a riser. Many researchers (11, 13) believe that the solid holdup profile in a riser has a S-shape with a dense zone at the bottom of the riser, a dilute phase at top of the riser and an inflection point dividing the two regions. However, the S-shape solid holdup profile was not observed in this study or other experiments (16, 17). In this study, the riser was divided into two sections, an acceleration zone and a fully developed zone equipped with a right angle exit. At a constant riser inlet velocity, solid holdup in a riser increased with increasing solid mass flux. From the right angle exit geometry in the riser in this study, a fully developed region emerged over a 1/2-riser height from the bottom in the two (0.009m-ID x 1.9 m-high and 0.0254m-ID x 4m-high) CFB risers. These results showed a similar trend to that of simple exponential decay type reported by Brereton and Stromberg (16), who used an abrupt exit, except for the top-section of the riser due to an end effect phenomenon.

Fig. 4 shows the effect of the solid mass flux on the mean solid residence time in a CFB riser. As shown, the average solid residence time in the risers (0.009m and 0.0254m-ID) ranged from 3.5 to 6 sec^{-1} and 4 to 8 sec^{-1}, respectively. The mean solid residence time in a riser decreased with increasing gas velocity. These trends are consistent with those reported by Smolder and Baeyens (12) and Harris et al. (13). In addition, the mean solid residence time in a riser decreased with increasing solid mass flux at a constant gas velocity. However, these results showed a different trend based on the experimental data reported by Smolder and Baeyens (12) and Harris et al. (13). At a constant velocity, the mean solid residence time in a riser increased with increasing solid mass flux based on the data reported by Smolder and Baeyens (12). and Harris et al. (13). This is because the back-mixing of solids in a riser is enhanced by the increased solid mass flux, which results in an increase in solid residence time (12). These contrasting results can be explained by the apparatus adopting a 0.009m and 0.0254m-ID, which is much smaller than that used by Smolder and Baeyens (12) and Harris et al. (13). Therefore, back-mixing, which is the down-flow of particles near the wall of the riser in our apparatus (0.009 m-ID x 1.9 m-high CFB), wasn't detected. The Kunii and Levenspiel model (14) was used to analyze the axial solid holdup profile in this study. In this model, as the riser height increases in the free-board zone, the axial solid holdup profile in a riser appears to have the form of a simple exponential decay type with a lower dense region and an upper dilute region. The calculated decay factor was determined based on the Kunii and Levenspiel (14) model using Eqs. (3) to (8).

Fig. 5 shows the calculated decay factor according to the Kunii and Levenspiel model (14) using Eq. (8) along with previous data for comparison. The decay factors in this study (0.009m and 0.0254m-ID) were in the range of aU_r = 3~7 and 2~4 sec^{-1}, respectively. Kunii and Levenspiel (14) reported that the decay factor was related to the riser inlet velocity, which is in the range of aU_r = 2~4sec^{-1} for the Geldart A particles. The previous data using Geldart A particles as a bed material are in the range of aU_r = 2~4 sec^{-1}. However, the experimental results using a 0.009m-ID CFB were higher than those previously reported data using Geldart A particles. This can be explained by upflow particle agglomerates in the narrow riser (0.009m-ID) with higher likelihood of moving to the wall of the riser and then changing the direction to the dense region in the riser (14). Also, the decay factor adopting a 0.0254m-ID was smaller than that adopting a 0.009m-ID. As the riser inlet diameter increased, the up-flow particle agglomerates had a lower probability than that of the smaller riser inlet diameter. This can cause a higher solid holdup in a dilute region, which results in a higher decay factor in a riser. Moreover, the decay factor in a riser appeared to increase with increasing particle diameter. This trend can be explained by agglomerates of the denser and coarser particles being more likely to the change direction and move the down flow in the dense region (14). In this study, the decay factor in a riser increased with increasing particle diameter from 53 to 90 μm. However, the decay factor using a 140 μm as the bed materials was lower than that of smaller particles (from 53 to 90 μm). The decay factor is dependent on the riser inlet velocity, solid mass flux and average solid residence time. Therefore, a lower solid mass flux ($37.08<G_s<53.87$ kg/m²/s) using 140 μm particles in this study caused a lower solid holdup and solid residence time, and decay factor in the riser represents lower value. The solid mass flux was ranged with $43.3<G_s<65.9$ kg/m²/s in the smaller particles (from 53 to 90 μm).

Fig. 6 shows comparison between measured solid holdup and predicted values with experimental variables in two CFBs and other studies (17, 25). Fig. 6(a) and (b) represent the axial solid holdup profile with the experimental variables in comparison with the correlations by Adánez et al. (19) and Lei and Horio (20) respectively. In addition, Bai and Kato (20) proposed Eqs. (11) and (12) to determine the solid concentration of the inlet and outlet of a riser. As can be seen, results of correlations reported by Adánez et al. (19) and Lei and Horio (20) underestimated the solid concentration in the dilute phase compared to the measured data of 0.009 m-ID x 1.9 m-high and 0.0254 m-ID x 4.0 m-high CFB. However, correlations reported by Lei and Horio (20) and Adánez et al. (19) well matched the solid concentration in the dilute phase compared to the measured data of 0.10m-ID x 9.3m-high CFB (17) and 0.10 m-ID x 16 m-high CFB (25).

Fig. 7 shows the prediction of solid holdup in a riser affected by exit geometry. As can be seen, prediction of solid holdup (this study and Kim et al. (28)) in Eqs. (14 and 15) shows a significant deviation. However, data from Pugsley et al. (29) are well matched the prediction of Kim et al.(27).

In this study, the empirical correlation was obtained for decay factor to estimate the axial solid holdup in a riser based on Eq (10) by Lei and Horio (20).

$$aD_r = 2.19\times10^{-3}\left[\frac{U_r}{\sqrt{gD_r}}\right]^{(-6.34\times10^{-2})}\left[\frac{U_r}{G_s/\rho_p}\right]^{0.23}\left[\frac{\varepsilon_{sd}}{\varepsilon_{se}}\right]^{0.567} \qquad (16)$$

With a correlation coefficient of 0.91 and standard deviation of 0.46x10^-3^. The range of variables for Eq. (16) covers $7.34 \le U_r/\sqrt{gD_r} \le 11.79$, $120.32 \le U_g/(G_s/\rho_p) \le 260.23$, $4.08 \le \varepsilon_{sd}/\varepsilon_{se} \le 6.53$.

Fig. 8 shows the prediction of axial solid holdup in 0.009m-ID riser and Kim et al. (28) data. The predicted axial solid holdup by previous studies (19, 20) at the bottom of riser was poorly predicted because of wall effect in small diameter in Fig. 6. Therefore, experimental data at the bottom of riser were adopted for the correlation of the decay factor. As can be seen in Fig. 8, the decay factor by proposed correlation predicts well in comparison with the Fig. 6.

CONCLUSION

This study examined the change in the axial solid hold-up profile in two CFBs (0.009m-ID x 1.9m-high and 0.0254m-ID x 4m-high). The axial solid holdup profile in a riser had a simple exponential decay type with two sections, an acceleration zone and a fully developed zone in a riser equipped with sharp right angle exit. The decay factors of the CFB-risers (ID: 0.009 and 0.0254m) calculated using the Kunii and Levenspiel

(13) model ranged from 1.52 to 1.96sec^{-1} and 0.59 to 1.29sec^{-1}, respectively. Based on the experimental results from two-CFBs, the decay factor in a riser was affected by the riser diameter. In addition, the experimental data of the axial solid holdup in the two CFBs were compared with the correlations and model equations of previous studies. Also, empirical correlation was proposed for decay factor that exhibited a good agreement with experimental data.

ACKNOWLEDGEMENTS

The authors wish to acknowledge the Korea Ministry of Knowledge Economy (MKE) for funding the "Project of next-generation novel technology development" of ITEP. This study was partly supported by the GRRC program of Gyeonggi province through a research program and instrumental support.

References

1. Das M, Meikap BC, Saha RK. Axial voidage profiles and identification of flow regimes in the risers of circulating fludized bed. *Chem. Eng. J.* 2008; 145: 32-43.
2. Gupta Sk, Berruti F. Evaluation of the Gas-Solid Suspension Density in CFB Risers with Exit Effects. *Powder Techol.* 2000; 108: 21-31.
3. Bai D, Kato K. Quantitative Estimation of Solid Holdups at Dense and Dilute Regions of Circulating Fluidized Beds. *Powder Techol.* 1999; 101: 183-190.
4. Matsen J. Design and scale-up of CFB catalytic reactors. Eds by Grace JR, Avidan AA, Knowlton TM. *Circulating Fluidized Beds*, London, 1997; 489-503.
5. Bai DR, Jin Y, Yu ZQ, Zhu JX. The axial distribution of the cross-sectionally averaged voidage in fast fluidized beds. *Powder Techol.* 2000; 71: 51-58.
6. Kwauk M. Ed. Fast Fluidization. Vol. 20, Advances in Chemical Engineering Series 1994.
7. Grace JR, Avidan AA, Knowlton TM. Reactor modeling and for high velocity. *Circulating Fluidized Beds*, 1997.
8. Berruti F, Chaouki J, Godfroy L, Pugsley TS, Patience GS. Hydrodynamics of Circulating Fluidized Bed Risers: a Review. *Can. J. Chem. Eng.* 1995; 73: 569-602.
9. Li Y, Kwauk M. The dynamic of fast fluidization, Eds. By Grace JR, Masten JM, *Fluidization,* 1980; 537-544.
10. Hartge EU, Li Y, Werther J. Analysis of the local structure of the two phase flow in a fast fluidized bed, Eds. By Basu, P. *CFB Techol*, 1986; 153-160.
11. Kato K, Shibasaki H, Tamura K, Arita S, Wang C, Takarada T. Particle holdup in a fast fluidzed bed. J. *Chem. Eng. Japan*. 1989; 22: 205-211.
12. Smolders K, Baeyens J. Overall solids movement and solids residence time distribution in a CFB-risers. *Chem. Eng. Sci.* 2000; 55: 4101-4116.
13. Harris AT, Davidsion, JF, Thorpe RB. *Chem. Eng. Sci.* 2003; 58: 2181-2202.
14. Kunii D, Levenspiel O. Entrainment of Solids from Fluidised Bed, *Powder Techol.* 1990; 61: 193.
15. Schnitzlein MG, Weinstein H. Flow Characterization in High-Velocity Fluidized Beds Using Pressure Fluctuations, *Chem. Eng. Sci.* 1988; 43(10): 2605.
16. Zhang H, Xie Y, Chem Y, Hasatami M, Basu P, Horio M, The radiative heat transfer of the immersed tube in a fluidized-bed. Eds by Hasatami, *CFB Tech.* 1991; 151.
17. Brereton C, Stromberg L. P. Some aspects of the fluid behavior of fast fluidized beds. Eds by Basu P, *CFB Techol*. 1986; 133.
18. Rhodes MJ, Geldart, D. The Hydrodynamics of Re-Circulating Fluidized Beds. Ed by Basu P. *CFB Techol*. 1986; 193.
19. Adanez J, Gayan P, Garcia-Labiano F, de Diego LF. Axial voidage profile in fast fluidized beds. *Powder Techol.* 1994; 81: 259-268.

20. Lei H, Horio MJ. A Comprehensive Pressure Balance Model of Circulating Fluidized Beds. *Chem. Eng. Japan*. 1998; 31: 83.
21. Bai D, Kato K. Quantitative estimation of solids holdups at dense and dilute regions of circulating fludized beds. *Powder Techol.* 1999; 101: 183-190.
22. Arena U, Cammarota A, Piston L. High Velocity Fluidization Behavior of Solids in a Laboratory Scale Circulating Bed. Ed by Basu P, in *CFB techol*. 1986; 119.
23. Kato et al. paper delivered at *Soc. Chem. Eng*. Japan annual meeting, April 1987.
24. Takeuchi H, Hirama T, Chiba T, Biswas J, Leung LS. A quantitative regime diagram for fast fluidization. *Powder Techol*. 1986; 47: 195–199.
25. Huang W, Zhu J*, Chin. J. Chem. Eng*. 2001; 9: 70~76.
26. Kunii D, Levenspiel O. *Powder Technol. 1995;* 84: 83.
27. Kim SW, Kim SD, Lee DH. *Ind. Eng. Chem. Res.* 2002; 41, 4949.
28. Kim JS, Tachino R,Tsutsumi, A. *Powder Technol.* 2008; **187**, 37-45.
29. Pugsley T, Lapointe D, Hirschberg B, Werther J. *Can J. Chem. Eng. 1997; 75: 1001.*

Table 1. Physical properties of bed materials.

Bed materials	$\overline{d_p}$,[m]	ρ_s , [kg/m^3]	U_{mf}, [m/s]	U_t, [m/s]	Geldart classification
FCC	52.8	1885.7	0.0026	0.18	A
	82.4		0.0050	0.28	
	89.9		0.0066	0.47	
	140.7		0.0111	0.86	

Table 2. Experimental variables and ranges.

	U_r ,[m/s]	U_{seal}/U_{mf} ,[-]	Inventory ,[kg]
(a) 0.009m-ID x 1.9m CFB	2.18~3.50	2.44~7.09	0.2
(b) 0.0254m-ID x 4m CFB	2.45~3.12	1.96~8.38	4

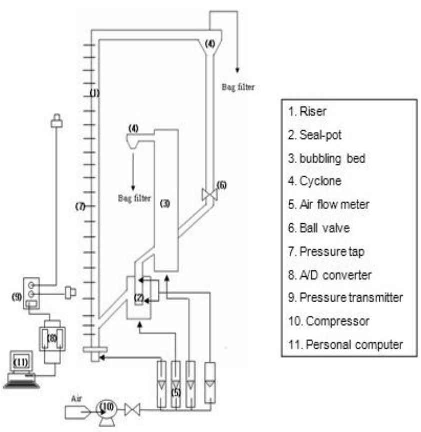

Figure 1. Schematic diagram of the experimental apparatus.

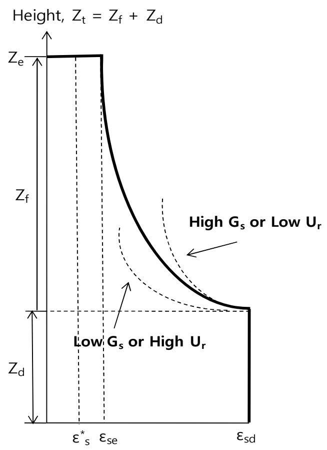

Figure 2. Axial solid hold-up in a fast fluidized bed from the entrainment model.

.

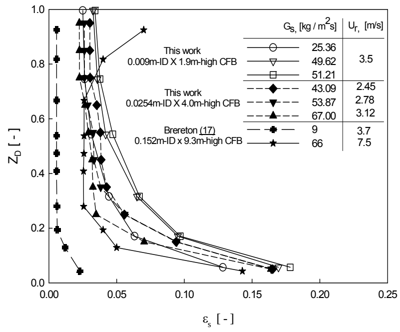

Figure 3.Variation of the axial solid hold-up profile with the experimental variables. The results of previous studies are shown for comparison.

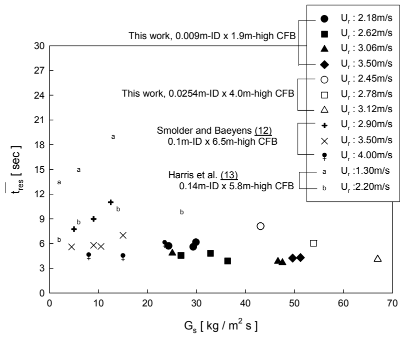

Figure 4. Effect of the solid mass flux on the average solid residence time in a riser. The data reported by Smolder and Baeyens (12), Harris et al. (13) are shown for comparison.

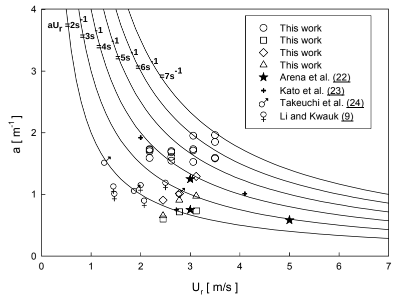

Figure 5. Calculated decay factor using the Kunii and Levenspiel model(14) in this study. The results of previous studies are shown for comparison.

Symbol	Authors	d_t (m)	Solid type	d_p (㎛)	U_r (m/s)	G_s (kg/m^{2}s)
○	**This work**	0.009	FCC	82	2.18~3.50	24.3~51.2
□	**This work**	0.0254	FCC	52.83	2.45~3.12	37~70
◇				89.89		
△				140.7		
★	Arena et al. (22)	0.041 0.12	FCC/glass	70	2.5~5	49, 120
+	Kato et al. (23)	0.066 0.097	FCC	61	2~4.4	48~50
♂	Takeuchi et al. (24)	0.1	FCC	61	1.7~2.9	8.3~79
♀	Li and Kwauk (9)	0.09	FCC/Alumina	54,58/58	0.8~2.1 / 2.2~4	73

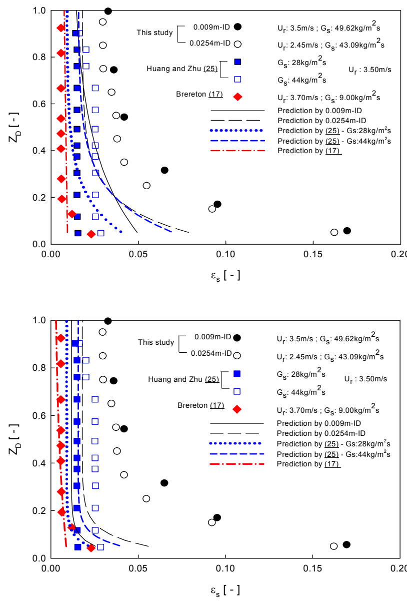

Fig.6.Comparison between measured solid holdup and predicted values with experimental variables in two CFB and other study(17, 25).
(a) Adanez et al. (19) (b) Lei and Horio (20) correlations.

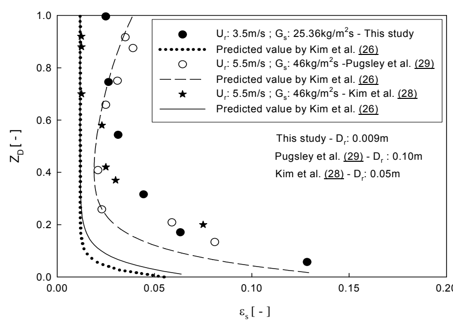

Figure 7. Comparison between measured solid holdup and predicted values with experimental variables in two CFBs affected by riser exit.

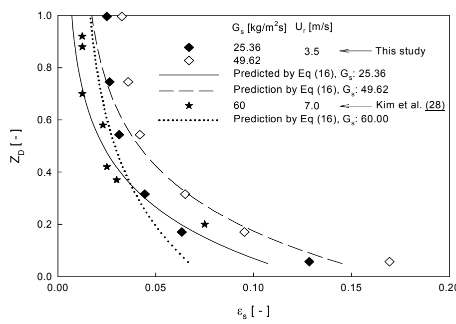

Figure. 8. Prediction of axial solid holdup in 0.009m-ID riser and data of Kim et al. (28) by proposed correlation.